

# Ion beam for synthesis and modification of nanostructures

D. K. Avasthi<sup>1,\*</sup> and J. C. Pivin<sup>2</sup>

<sup>1</sup>Inter University Accelerator Centre (IUAC), Post Box 10502, New Delhi 100 067, India

<sup>2</sup>Centre de Spectrometrie Nucleaire de Spectrometrie de Mass (CSNSM), Batiment 108, 91405, Orsay Campus, France

**The role of energetic ions of energies from a few keV to hundreds of MeV in nanostructuring is highlighted with the examples of nanostructures obtained by ion irradiation experiments at Inter University Accelerator Centre (IUAC), Delhi and Centre de Spectrometrie Nucleaire de Spectrometrie de Mass CSNSM, Orsay. They range from the use of ion or atom beams of a few keV to generate periodic ripples on surface or grow nanocomposite thin films by sputtering to the formations of anisotropic structures under swift heavy ion impacts. Swift ion irradiation of polymers or fullerenes creates strings of carbon particles or wires useful as nanocontacts or field emission tips. The elongation of noble metal particles embedded in insulators attracts attention for the design of light filters or waveguides. The swift heavy ion irradiation of silica film containing Fe nanoparticles, transforms the magnetic easy axis from in-plane to out-of-plane, which is of relevance to the perpendicular magnetic recording of information.**

**Keywords:** Ion beam thin films, nanostructures, nanoparticles.

NANOSTRUCTURED materials attract the attention of materials scientists because their extremely small size and large surface-to-volume ratio lead to size dependent chemical and physical properties, quite different from those of bulk materials of the same chemical composition<sup>1-3</sup>. The critical size of the nanodomains with particular properties is defined on the basis of relevant dimensions in each branch of physics, such as the Bohr radius of excitons in semiconductors or the correlation length of spins in magnets. The wide range of promising applications of nanomaterials have led to tremendous research activities in this field. Nanoparticles are nowadays considered to be useful building blocks for future technologies. The most common and economical approach of generating nanostructures is the chemical route. However, for many applications, thin films are required, which are sometimes not achievable by chemical techniques. The other methods of creating nanostructured thin films are vapour phase condensation (and co-condensation), arc discharge, RF plasma sputtering (and

co-sputtering), ion beam sputtering, ion implantation and other ion-beam based methods, pulsed laser deposition, etc. One can distinguish two basic approaches in synthesis of nanostructures as bottom up and top down. In bottom up processes, the atoms are brought together to form particles of nanometric dimension whereas in top down processes, large size grains are broken to form nanodomains. Both are used in the ion beam based methods.

Ion irradiation is a particularly suitable means to create or modify nanostructures, since ions with low energies (in the range where the energy loss is dominantly via elastic collisions) induce a collision cascade on a shallow thickness of the material and high energy ions perturb the structure of the target in narrow channels (with diameters of the order of 10 nm) up to a few microns in depth, mainly through electronic energy transfer processes. In addition, the nanopatterning of thin films can be achieved by a focused ion beam. The induced transformations are often unusual, because of the short duration of the interaction, typically of  $10^{-13}$  s for the cascade and of  $10^{-12}$  and  $10^{-10}$  s for the relaxation of the lattice and electron gas. As a landmark, the swift heavy ions (SHI) are those with a velocity comparable or larger than the orbital electron velocity and their energies are typically about or more than 100 keV/amu. SHI have the unique feature of depositing a large energy density per unit length ( $S_e \sim 10$  keV/nm), which is for instance liable to produce an amorphization of the target material in the perturbed cylinder along the ion path, which is referred to as ion track. A transient melting or vapourization of the material is assumed to occur beyond a threshold of energy transfer to the electronic system<sup>4</sup>. On the other hand, transformations in the ballistic regime may result from the disordering correlated to the atomic displacements or from local changes of compositions, because of the diffusion of atoms during the cascade (radiation induced) or of residual defects (radiation enhanced), when the latter are mobile at the temperature of the experiments. The topology of the target surface is also affected by these various types of events and by the ejection of atoms (sputtering).

This review discusses the possibilities offered by ions of different energies in nanostructuring of materials. The energy loss of ions in the material can be either by elastic collisions or by inelastic collisions, which is quantitatively governed by the ion mass and its energy, and can

\*For correspondence. (e-mail: dka4444@gmail.com)

be determined by means of TRIM code simulations of ion impacts<sup>5</sup>. The electronic energy loss,  $S_e$ , dominates at high energies (>100 keV/nucleon) and nuclear energy loss,  $S_n$ , at low energies (<10 keV/nucleon) and ions of heavier mass have higher energy losses (nuclear as well as electronic). Nevertheless, applications can be sorted in correspondence with three energy ranges, for example, (i) very low energies up to a few keV suitable for sputtering purpose, (ii) energies from tens of keV to a few MeV used in implantation and ballistic mixing experiments and (iii) energies above 100 keV/nucleon used for creating linear tracks. Figure 1 gives an outline of the typical behaviour of the low- and high-energy ions in materials.

The important issues concerning the properties of nanomaterials are the control of (i) the mean size of particles, (ii) the particle size distribution, (iii) their filling factor in the structure and (iv) the creation of special structures, such as an alignment of the particles along the ion tracks, a tilting of the easy magnetization direction in films, etc. Examples of ion beam synthesis of nanostructures have been selected mainly from investigations of our group, and other related works, for discussing the underlying mechanisms and outlining some rules which can be used for applications. The present article is a review of the research work carried out by our group (Inter University Accelerator Centre (IUAC), Delhi and

Centre de Spectrometrie Nucleaire de Spectrometrie de Mass (CSNSM), Orsay) in the field of nanotechnology by ion beams, covering energy range from a few keV to a few hundred MeV.

### Nanostructuring with low energy ions (a few keV)

#### *Creation of nanoripples and other surface nanostructures*

The creation of periodic arrays of nanoripples and nanodots by sputtering with low-energy ions in metals and semiconductors has been reported by various groups<sup>6-10</sup>. The practical interest in building nanoripples at the surface of targets is that they can further act as templates for growing nanowires in the groves. The surface relief induced by sputtering under certain conditions can take the shape of ripples similar to those created by the wind on the sea or the sand. The ion energies of interest for creating defects close to the surface range from a few hundred eV to a few keV. Nevertheless, energies up to a few hundred keV have also been used. The mechanism is of complex nature<sup>6</sup>, involving the roughening by sputtering and the surface reconstruction by diffusion processes, and the final morphology is determined by the balance between the two. Cuerno *et al.*<sup>7</sup> proposed a stochastic model to express balance equations. The periodic ripples can be formed either perpendicular or parallel to the projection of the ion beam direction in the surface plane depending on the ion incidence angle.

The originality of the work performed at IUAC was to use atom beam instead of ion beam to create ripples at surface on Si crystal surface<sup>8</sup>, which is important for creating ripples specially at the surface of insulators. The dependence of the ripple wavelength on atom fluence and on the orientation of Si surface was studied. Figure 2 shows the ripples at the surface of Si(100) and Si(111) wafers, bombarded by 1.5 keV Ar atoms at a fluence of  $3.4 \times 10^{17}$  ions/cm<sup>2</sup>.

#### *Synthesis of metal particles and semiconducting particles in insulating matrix by atom beam sputtering*

A set-up for atom beam sputtering has been designed and assembled at IUAC as shown in Figure 3<sup>11</sup>. The choice of an atom beam source instead of an ion source has the advantage that a neutral beam does not produce charging of the surface of insulating targets by ejection of secondary electrons. It can be used for building surface nanostructures on a target (previous section) as well as for depositing nanocomposite thin films. Our set-up consists of an atom source connected to a vacuum chamber pumped by a turbomolecular pump, a motionless target and a substrate holder, which can be rotated at slow speed so as to get uniform deposition.

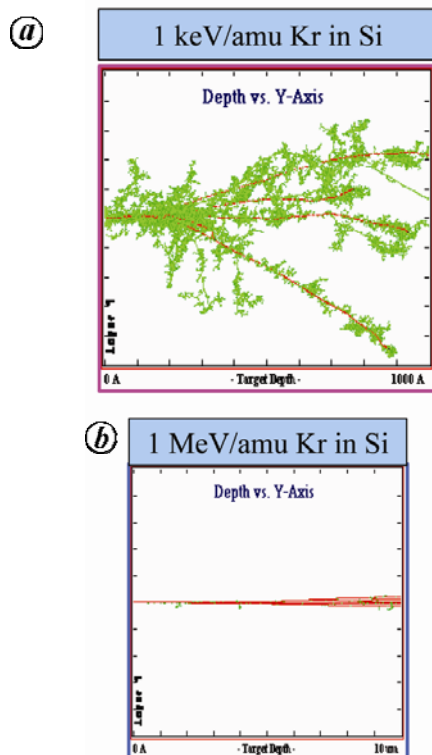


**Figure 1.** SRIM simulations of five ion impacts showing that *a*, in nuclear slowing down regime the trajectory of ions is not exactly straight and secondary collisions occur, whereas *b*, in case of swift ions, the ion paths are straight except at the end of range of ion.

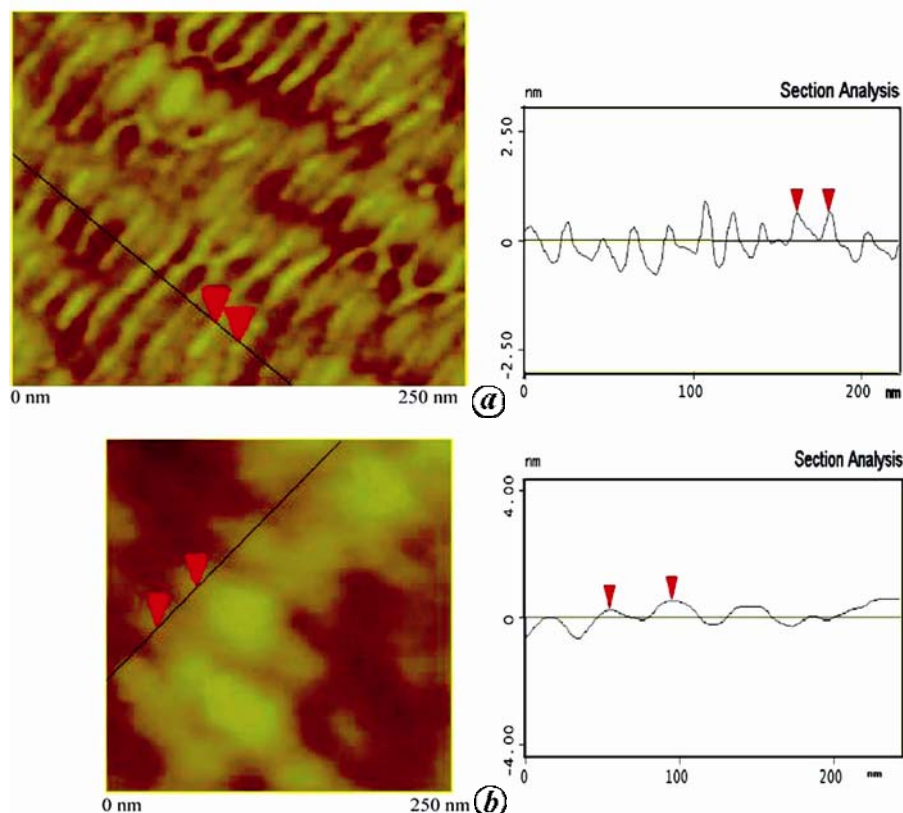


**Figure 2.** AFM images show nanoripples on Si single crystal (100) irradiated with 1.5 keV Ar atom at two different fluences<sup>8</sup>.

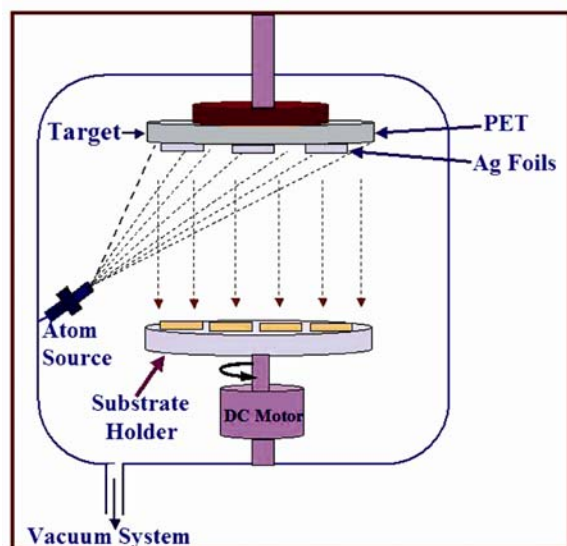


**Figure 3.** A schematic sketch of the atom beam sputtering set-up<sup>8,11</sup>.

The design of the source is such that the produced ions are neutralized after extraction. If neutralized before extraction they cannot be accelerated. The set-up has been used to synthesize films made of noble metal particles or semiconducting particles embedded in insulating matrices such as silica<sup>12</sup>, carbon<sup>13</sup> and polymer<sup>14</sup>, etc. The

structure of the thin composite films has been characterized by various techniques, including transmission electron microscopy (TEM) and atomic force microscopy (AFM). The Ag-polymer nanocomposites (Figure 4), synthesized by atom beam deposition have been shown to exhibit interesting optical properties<sup>14</sup>. Indeed, the fractal network of Ag nanoparticles (Figure 4a) has a broad absorption band, extending up to infrared region (Figure 4b), which is useful for absorbing solar energy more efficiently. Their narrow transmission window around 320 nm can also find technological application as UV filters. The uniformity of metal nanoparticles distribution at the scale of a few cm<sup>2</sup> obtained by co-evaporation and by atom beam sputtering has been compared and proves to be better in the second case<sup>11</sup>. Furthermore, the precipitation of nanoparticles in the coating without annealing is obtained more easily, most probably because the sputtered atoms hit the substrate with energies of a few eV instead of about 0.1 eV for evaporated atoms. Other processes such as pulsed laser deposition also provide beams with noticeable kinetic energies but it must be stressed that they do not permit deposition of homogeneous films over several cm<sup>2</sup>. Thin films made of ZnO: Au were also deposited<sup>15</sup> by atom beam co-sputtering and submitted to subsequent annealing, as it is known that noble metals catalyse the growth of ZnO nanorods<sup>16</sup>. A few nanorods obtained with our set-up are shown in Figure 5.

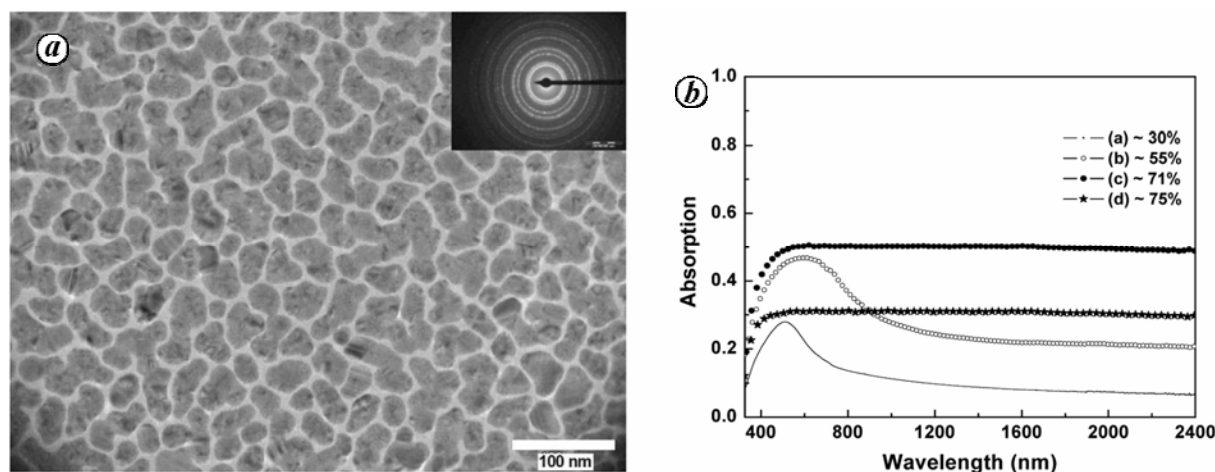


**Figure 4.** *a*, TEM micrographs of Ag-PET nanocomposite is shown, which has Ag about 71 at.%. The corresponding diffraction rings are shown in the inset. Dark region represents the metal and the bright region represents the polymer. *b*, The optical absorption spectra of Ag-PET nanocomposites (*a* to *d*) in visible and in infrared (IR) region, show the broad absorption extending in IR region<sup>14</sup>.

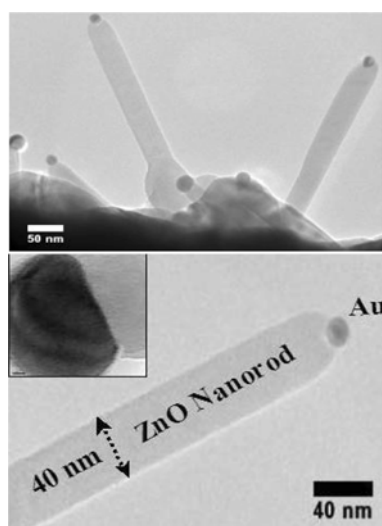


**Figure 5.** The TEM viewgraphs of the ZnO nanorods with Au particle at top grown by the annealing of the atom beam co-sputtered sample of Au–ZnO (ref. 15). One of the pictures shows a ZnO nanorod with Au nanoparticle at top.

### Synthesis of nanoparticles by ion implantation

Ion implantation is the most versatile means to introduce a foreign element A in the near surface region of a solid B, for the purpose of modifying the electronic structure by addition of a doping element in low concentration or for obtaining a supersaturated solid solution. As A and B are seldom soluble in all proportions, particles of pure A phase or of a compound  $A_xB_y$  are liable to form in the course of the implantation process whenever atomic defects are mobile at the implantation temperature, otherwise the implanted samples have to be submitted to a subsequent annealing. This thermal treatment is also generally required for restoring the structure of the matrix, as all

semiconductors and many covalent or ionic compounds are amorphized by the collision cascades produced by implanted ions. Metals implanted with another metal species remain generally crystalline, apart for selected composition of metallic glasses, but a dense network of dislocations is developed. The implantation may be performed at temperatures significantly higher than the ambient, or the beam current can be increased as much as possible for favouring the dynamic annealing of the defects and growth of particles by radiation enhanced diffusion. Such conditions of implantations lead to epitaxy relationships between particles and matrix when the reticular distances are comparable in some crystallographic planes. Favourable cases are, for instance, particles of Ge in SiC<sup>17</sup>, Fe particles in Ge<sup>18</sup> or particles of metal oxide, carbide or nitride by implantation of O, C, N in a metal<sup>19–21</sup>, because the compound lattice is generally built by insertion of the metalloid atoms in the host matrix.

The nature of the precipitated phase obtained by dynamic annealing at temperature  $T_i$  or implantation at low temperature  $T_j$  followed by annealing at same temperature  $T_i$  is often different, if the matrix undergoes a recrystallization between  $T_j$  and  $T_i$  (refs 22–24). Many papers concern the synthesis of particles of noble metals, Ag, Au or Cu or their alloys because of their interesting surface plasmon resonance<sup>25,26</sup>. Figure 6 shows a TEM picture of Ag particles in silica matrix synthesized by implantation<sup>27</sup> of Ag ions at fluence of  $1.6 \times 10^{16}$  ions/cm<sup>2</sup>. The Ag concentration at the mean range of implanted ions is of 5 at.%. There is always a broad size distribution of particles formed by ion implantation because of the depth gradient of the implanted atoms. In the case of silica implanted with Ag ions, this problem gets worse with the increasing fluence. As a consequence of the variations in size and in interparticle distances with depth affecting the mutual polarization of the particles, the surface plasmon

resonance of such a system becomes broader with the increasing concentration of implanted atoms.

#### Limitations and possible solutions

The synthesis of nanoparticles by ion implantation poses mainly three problems. First, when ions are implanted at low energies, their depth profile intersects the surface so that incoming ions sputter previously implanted ones. When the fluence is increased, the concentration of implanted element saturates. Next, if the ions are implanted at higher energies (to overcome problem of sputtering of implanted atoms), the duration of the implantation may be prohibitive because the concentration at the mean range decreases in inverse proportion to the profile width, which varies almost in proportion to the ion energy. Finally, the size distribution of the formed particles is not uniform due to the concentration depth gradient of implanted atoms.

Some efforts are made to achieve a narrower size distribution in nanoparticles synthesized via implantation by performing a subsequent irradiation with SHI then annealing. The underlying idea is that each SHI produces defects over a certain diameter which will help to limit atomic diffusion to the same region during annealing. The formation of Si nanoparticle with a narrower size distribution in silica implanted with Si ions has been reported by Mohanty *et al.*<sup>28</sup>. One can also perform implantations at different energies to achieve a more uniform concentration of implanted atoms.

#### Synthesis of nanoparticles by ion beam mixing

The basic mechanisms involved in mixing of multilayers by ions in ballistic regime are collision cascades, recoil

implantation and radiation enhanced diffusion. This ballistic mixing can lead to the formation of nanoparticles in non-miscible systems such as layers of noble metals embedded in matrices made of Si, SiC, SiO<sub>2</sub>, Al<sub>2</sub>O<sub>3</sub> and other ionic insulators<sup>29,30</sup>. In these systems, the radiation enhanced diffusion of metal atoms, displaced by cascades leads to a spheroidization of the metal layer for minimizing the interface energy. In addition, the metal atoms which are displaced by recoil implantation at too large distances for returning to the surface of these 'macroparticles' form satellite particles with smaller size<sup>31</sup> arranged in a concentric halo around the central 'macroparticle' (Figure 7), contrary to the case of implantation (Figure 6). This particular arrangement leads to a screening of dipolar interaction between the macroparticles: the spherical halo of nanoparticles acts on the local electric field as a uniform charge distribution  $\rho$  at the surface of a sphere<sup>32</sup>.

#### Nanostructuring under the effect of electronic excitations

##### Formation of C nanodots in polymers

Molecular solids are highly sensitive to ionizing radiations of any type. The interest of using ion beams for creating radicals and subsequent chemical transformations lies in (i) the much higher radiolytic efficiency of ions<sup>33,34</sup> and (ii) in localizing the chemical transformation within narrow cylinders. Ions induce a more selective release of H from molecules than electrons or photons, resulting in more localized crosslinking of the bonds and collapse of the molecular structure into an amorphous network of a-C:H.

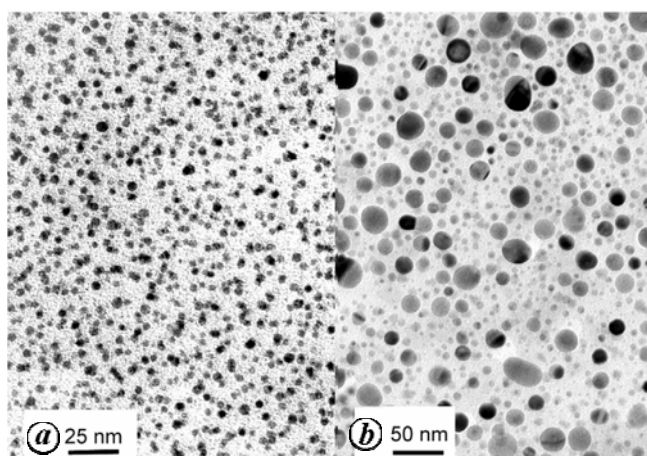


**Figure 6.** TEM images show Ag nanoparticles synthesized by ion implantation with (a)  $10^{16}$  and (b)  $10^{17}$  Ag/cm<sup>2</sup> of 150 keV. For the fluence of  $10^{16}$  atoms/cm<sup>2</sup> (a), the size of the formed clusters is quite uniform with a mean value of 1.4 nm and a standard deviation of 0.5 nm. For the fluence of  $10^{17}$  atoms/cm<sup>2</sup> (b), the frequency of clusters decreases monotonically with increasing size, ranging from 2 to 20 nm. The arithmetic mean is 9 nm (ref. 27).

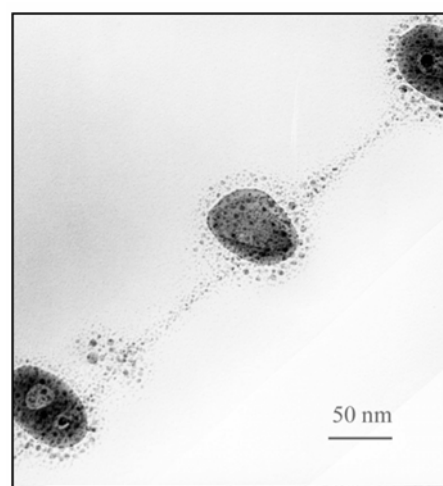


**Figure 7.** TEM (cross sectional) images of metal nanoparticles formed by ion beam mixing of a SiO<sub>2</sub>/Ag 8 nm/SiO<sub>2</sub> film ion beam mixed with  $1.6 \times 10^{16}$  Au ions. Dual distribution of particles (formed by spheroidization of the layer and by recoil implantation) is clearly visible. Large size particles are surrounded by small size particles<sup>30</sup>.

In the case of inorganic polymers and gels (polymers with disordered chains formed from solutions of organic precursors like alkoxides), consisting of metal–oxygen or metal–carbon chains with organic side groups, irradiation with ions of any energy induces the segregation of C from organic groups into clusters. When the concentration of organic group and irradiation fluence are limited, the clusters do not grow too much so that they are semiconducting and exhibit confinement. It is worth noting that atomic collisions play no role in all these transformations (H release, crosslinking and C segregation) and their yield is directly proportional to the integrated amount of electronic excitations<sup>35</sup>. Figure 8 shows the C nanodots formed by irradiation with 3 MeV Au ions of a gel with composition  $[\text{Si}(\text{CH}_3)(\text{H})\text{-O}]_n$  derived from methyltriethoxysilane  $(\text{Si}(\text{CH}_3)(\text{OC}_2\text{H}_5)_3)_n$ . Images of the C distribution in a cross-section of the film were obtained<sup>36</sup> by energy filter TEM. In this case, the C clusters are randomly scattered in the film because the used ions also underwent nuclear collisions deviating from their trajectories.

In the case of irradiation with swift ions, having a straight path in the material, the C clusters become aligned in strings<sup>37</sup>. Raman analyses show however that, whatever their arrangement and percolation in tracks, the C clusters exhibit a noticeable degree of  $\text{sp}^3$  hybridization, while percolation should increase the proportion of  $\text{sp}^2$  bonds taking into account the known effect of the cluster size on the probability of graphitic loops<sup>38</sup>. C clusters are also formed in films of same nature by annealing in vacuum but they are made of turbostratic graphite.

Whatever the condition of irradiations, the clusters have comparable sizes for a given local density of transferred energy  $S_e\phi$  (where  $S_e$  is the stopping power and  $\phi$  the fluence). They are sufficiently small for exhibiting an excitonic confinement and they emit a yellow green

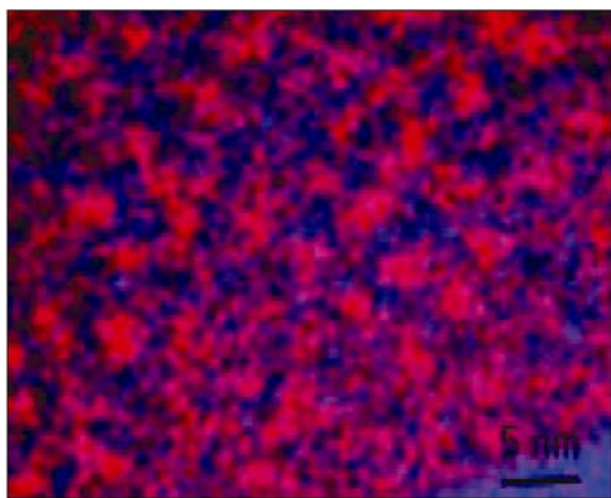


**Figure 8.** EFTM picture of carbon clusters aligned in track after irradiation of MTES by 3 MeV Au ions at a fluence of  $10^{15}$  ions/cm<sup>2</sup> (ref. 36).

luminescence, in contrast to the more graphitic particles formed during heat treatments. The emission peak shifts to the red with increasing irradiation fluence, due to the particles growth, and the luminescence yield shows a maximum for a given value of  $S_e \times \phi$ , beyond which the luminescence is quenched as excitons show no more confinement. Beside interesting optical properties, the irradiated films have 2–3 times higher hardness than that of heat-treated films, as shown by nanoindentation tests. The hardness of irradiated polycarbosilanes reaches that of bulk SiC.

Similar results have been obtained in several Si-based gels and polymers. For instance, C nanowires<sup>37,38</sup> have also been found in SHI irradiated organic polymers by Shu Seki *et al.*<sup>39</sup>.

#### *Precipitation of metal particles in gels and oxides*

When metallic ions  $M^{n+}$  are introduced in gels from triethoxysilane (in the form of salts), ion irradiation induces an oxidation–reduction process of these ions by the Si atoms with dangling bonds resulting from the radiolysis of Si–H bonds, instead of the formation of Si particles<sup>35,39</sup>. A threshold amount of energy is required to reduce sufficient M atoms in order to form stable nuclei. When the incident ions have a low electronic stopping power, an overlap of the tracks is needed and the precipitation kinetics obeys the same Poisson law as that of Gibbons model<sup>40</sup> for the formation of amorphous clusters in semiconductors within ballistic regime. Their size distribution remains very narrow as long as the source of metal ions in solid solution is not exhausted and the mean value can be as small as 2 nm<sup>41</sup>.

In other metastable systems such as silicate glasses containing Ag or Au solute atoms, a single ion impact is needed to form a stable nuclei even with He ions of a few MeV with an electronic stopping power of the order of 30 eV/Å (ref. 42). Therefore the precipitation kinetics is in this case simply a linear function of the transferred energy  $S_e\phi$  per unit length. The example of the precipitation of Ag particles in a sodalime glass by He ions is shown in Figure 9. The interesting characteristics of the particles formed is again their narrow size distribution and mean size (0.5–2 nm), compared to that obtained by annealing treatments at high temperatures of same materials.

Energetic ions deposit enough energy for reducing Fe ions in Fe–silica system<sup>43</sup>. The solubility of Fe in silica films grown by low-temperature processes such as magnetron sputtering (involving the deposition of atoms with low kinetic energies), is so high that only 2 at.% Fe is precipitated in films containing an overall concentration of 14 at.% Fe. Irradiation with SHI, such as for instance 100 MeV Au, proves to be more efficient than a thermal treatment at high temperature under Ar:H<sub>2</sub> atmosphere for reducing the Fe ions, since a reduction yield of

12 at.% in a film, containing 14 at.% Fe is achieved as against 4.5 at.% by annealing at 900°C. Beside their narrow size distribution obtained by the SHI irradiation in such systems, another interest is their alignment along the ion beam direction<sup>44</sup>. Such a structure is attractive for the perpendicular magnetic recording.

#### *Precipitation of Si nanoparticles in Si suboxide*

Thin films of SiO<sub>x</sub> were irradiated with SHI<sup>45</sup>, as a result of which the formation of Si nanocrystals was observed. The precipitation of Si nanoparticles was investigated on basis of the photoluminescence properties and TEM observations. It is expected that irradiation causes the evolution of oxygen from the film and a phase separation changes the system into Si nanocrystal and a more stoichiometric SiO<sub>2</sub> matrix. This is an interesting example of phase separation of Si and silica under dense electronic excitation due to reduction process.

#### *Creation of carbon nanowires in fullerene*

Fullerenes are almost as sensitive as polymers to irradiation of any nature and undergo similar transformations of crosslinking and amorphization. Therefore one may expect that isolated tracks in fullerenes constitute conducting path in an insulating matrix, if the disordering is continuous and the degree of sp<sup>2</sup> hybridization is large enough. Indeed, SHI irradiation of a fullerene film leads to local increase of conductivity, evidenced by AFM

imaging in conducting mode. Figure 10 shows the conducting paths observed<sup>46,47</sup> in a film irradiated with 120 MeV Au ions at a fluence of  $6 \times 10^{10}$  ions/cm<sup>2</sup>. The number of conducting paths is less than the ion fluence, indicating that some paths are interrupted. The threshold voltage for recording an electric signal decreases with the increasing ion mass and stopping power and the conducting paths diameter increases. These characteristics are all in agreement with the fact that a threshold of electronic energy transfer is required for promoting a transformation. When the linear density  $S_e$  is slightly lower than the threshold value, clusters of transformed matter are scattered along the ion path, and when it is higher, the transformed volume becomes a continuous cylinder. Now the increase in the diameter of conducting channels and the diode-like shape of the current-voltage curve are ascribed to the dual nature of the transformation occurring in the tracks. Vibrational spectroscopies put into evidence a polymerization of the fullerene at low ion fluences, vanishing as tracks overlap for being replaced by the formation of amorphous carbon. We attribute the conductivity in isolated tracks at low voltage as due to variable range hopping between amorphous carbon clusters formed in the tracks core and the steep increase of the conductivity at higher voltages to a contribution of polymerized phase formed in the tracks halo. Anyway, the diameter of the conducting channels can be tuned by choosing the mass and energy of the ions and they constitute efficient fields emitters<sup>48</sup>.

#### *Etched tracks and nanoripples as templates for nanostructures*

The modified zone in the ion tracks, especially in polymers, can be chemically etched out preferentially to obtain a chosen areal density of nanopores from a single one to a few 10<sup>11</sup>/cm<sup>2</sup> and with controlled diameters depending on membrane nature and ion stopping power. These track etched porous membranes can then be used as filters and sensors when functionalized by grafting other molecules inside or as templates to grow nanocylinders or nanotubes of desired materials, for controlled drug release, etc.<sup>49-54</sup>. Figure 11 shows the nanometer size ripples<sup>55</sup> formed at the surface of a NiO film on different substrates, irradiated at glancing angle by SHI at LN<sub>2</sub> temperature. The formation of such ripples is attributed to a dewetting of NiO with the Si and thermally grown silicon oxide on Si substrates<sup>55,56</sup>. These ripples can also act as templates for growing nanowires on the surface.

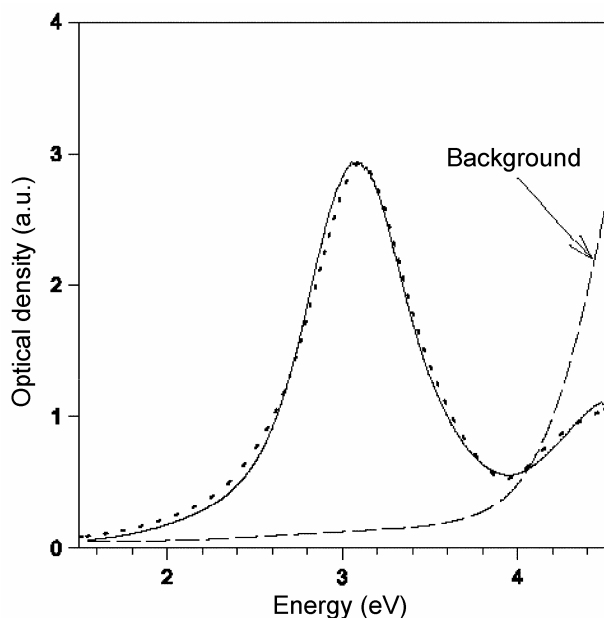


**Figure 9.** Optical absorption spectrum of Ag nanoparticles induced by 3 MeV He ion irradiation at a fluence of  $1 \times 10^{16}$ /cm<sup>2</sup> in a glass exchanged for 2 days in a bath containing 0.04 mol% AgNO<sub>3</sub> (continuous line). The spectrum has been corrected for the absorption of defects in the matrix shown by dashed line. The dotted line is a simulation for isolated particles based on Mie theory, for a particle size of 1.075 nm in a matrix with refractive index of pure silica<sup>42</sup>.

#### **Modification of nanoparticles under dense electronic excitation**

Little is known of the dissipation mechanism of the energy deposited by ions in composite materials. Simula-

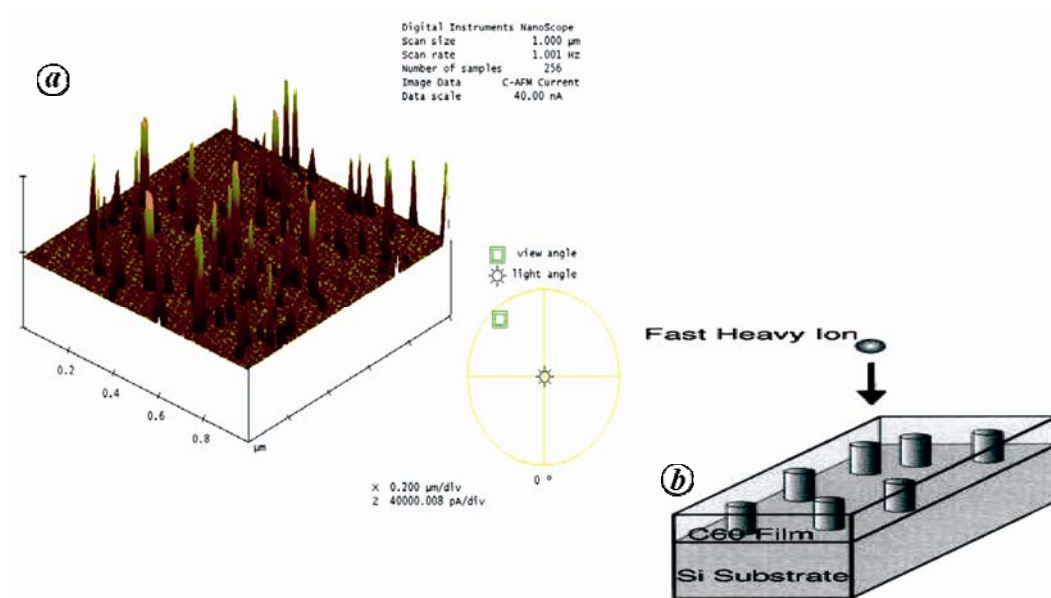


**Figure 10.** *a*, Conducting AFM image of the swift heavy ion (SHI) irradiated thin fullerene film. *b*, The fullerene film on substrate having the ion tracks created by SHI irradiation. The ion tracks are conducting due to the transformation of fullerene in conducting carbon<sup>46</sup>.

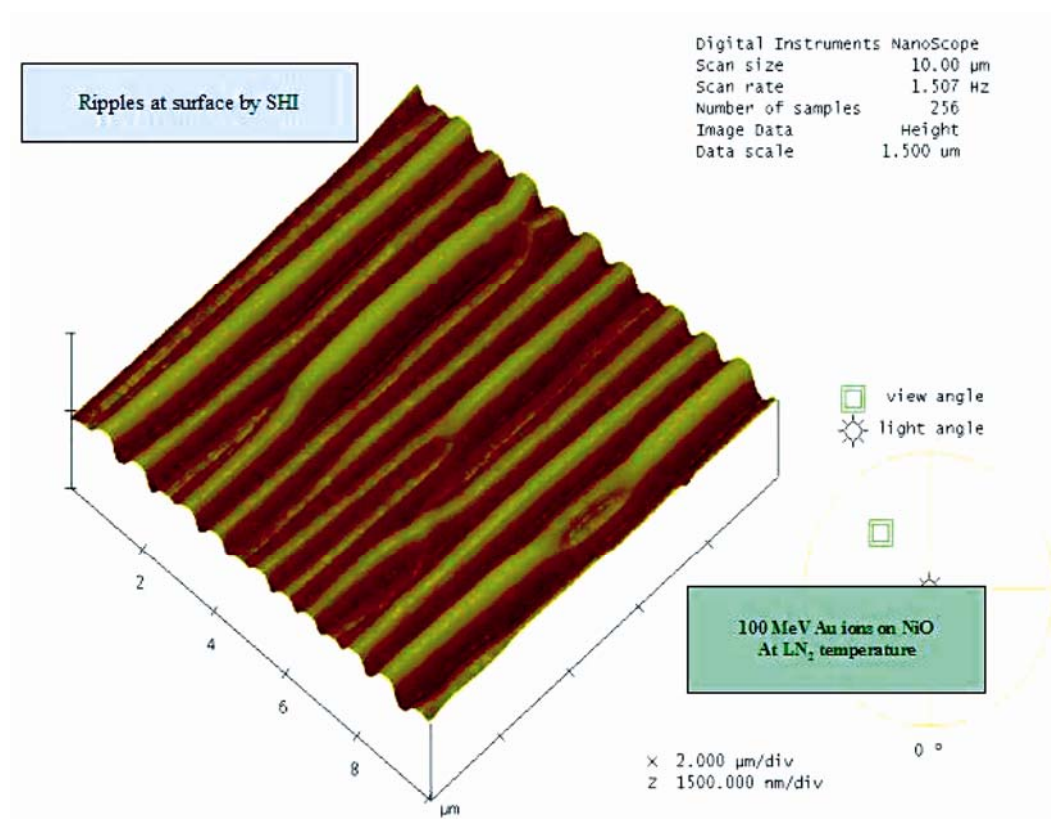


**Figure 11.** Ripples in NiO, obtained by 100 MeV Ag ion irradiation at glancing angle at liquid nitrogen temperature are shown here.

tions of thermal spikes have been undertaken recently for nanoparticles embedded in a matrix<sup>44</sup>. It has been shown that, when the nanoparticles are made of a metal with a relatively low melting point and a good thermal conductivity and the matrix is a refractory insulator, the heating

of the matrix facilitates the particle melting, whereas the bulk metal is known to remain unaffected under ion irradiation in same conditions. The simulations show that particles of Ag or Au are melted more easily than Fe particles of comparable size embedded in a silica matrix and

that all the more as they are small. When the particles have a size comparable to the diameter of the track in the oxide, they show an overheating at their periphery, liable to explain some of the experimental results reported in the next section.

An experimental investigation of these phenomena was undertaken at IUAC for correlating changes in noble metal silica nanocomposites to such calculations. Some structural modifications at the nanometric scale induced by SHI irradiation, are discussed<sup>57</sup>.

### Change of size and shape of Au and Ag nanoparticles under SHI irradiation

Au nanoparticles grown in teflon matrix by tandem thermal deposition (sequential deposition of thin Au and polymer layers), do not have spherical shape as evidenced by TEM observations. Films deposited directly on TEM grids were irradiated by 100 MeV Au ions at different fluences. It was observed<sup>58</sup> that the shape of particles became more spherical and their size grew with fluence. The spheroidization of the particles seems to corroborate the occurrence of transient melting. The average size of the nanoparticles, of about 9 nm before irradiation, became around 14 nm after irradiation. Therefore, it appears that the particles coalesce together to form bigger particles under SHI irradiation. Similar experiments were conducted on teflon films containing Ag nanoparticles. A quite different behaviour was observed compared to the case of Au nanoparticles, since a slight reduction of the particle size was observed instead and a loss of Ag atoms contained in the films was also evidenced by RBS. The latter fact indicates clearly the occurrence of electronic sputtering, for Ag nanoparticles in silica and it was not observed for Au particles in the same matrix<sup>59</sup>. Nevertheless, the occurrence of electronic sputtering for Au particles embedded in silica has been reported in another study<sup>60</sup>. On the other hand, surprisingly high sputtering yields were measured for very thin Au films on float glass under SHI irradiation<sup>61</sup>.

In another series of experiments, *in situ* X-ray diffraction (XRD) was used to take the snapshots (Figure 12) of the growth of the Au particles in silica matrix<sup>62</sup> from an average diameter of 4–9 nm under irradiation by 90 MeV Ni ions. Such a growth could be observed only for particles with an initial size smaller than the diameter of tracks and a high volume fraction (around 15%). When irradiating Au nanoparticles with a same volume fraction but larger sizes (mean diameter 12 nm) another phenomenon was observed, consisting in an asymmetric growth (along the beam direction) of some of the particles at the expense of smaller ones<sup>63</sup>. Figure 13 gives a cross-sectional TEM picture of the irradiated Au–silica nanocomposite, showing the elongation of Au nanoparticles along the beam direction. A similar elongation was found

for Ag nanoparticles with comparable mean size and volume fraction<sup>44</sup>. In both cases of Au and Ag nanoparticles, the elongation of the particles has an important implication for their surface plasmon resonance (SPR). Because of the larger value of the polarizability of particles parallel to their long axis, the SPR is shifted to red when the electric field of incident light is polarized parallel to the projection of the ion beam in the surface plane, SPR is shifted to the blue. The SPR absorption shows a dichroism of technological interest for light filters and waveguides.

A similar splitting of SPR is obtained by aligning the particles along the beam direction. This type of transformation has been observed for other filling factor (about 6 vol%) and size of Ag nanoparticles (varying from 2 to 15 nm) in a silicate glass, together with other

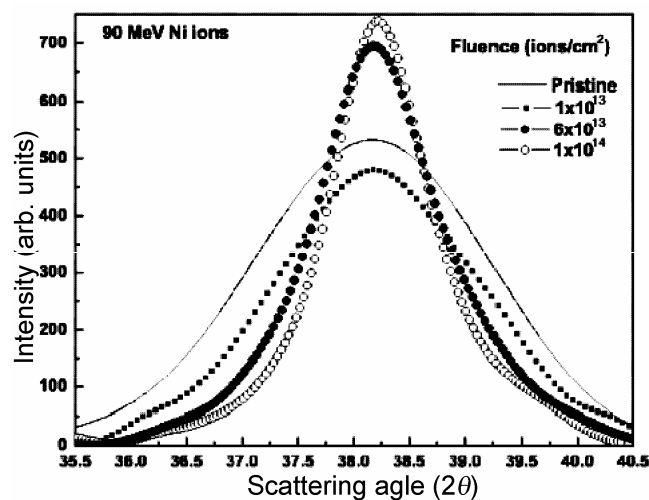


**Figure 12.** Ripening of Au particles in silica matrix (with 19 at.% metal fraction) by 90 MeV Ni irradiation as observed by *in situ* XRD, is shown here<sup>62</sup>.

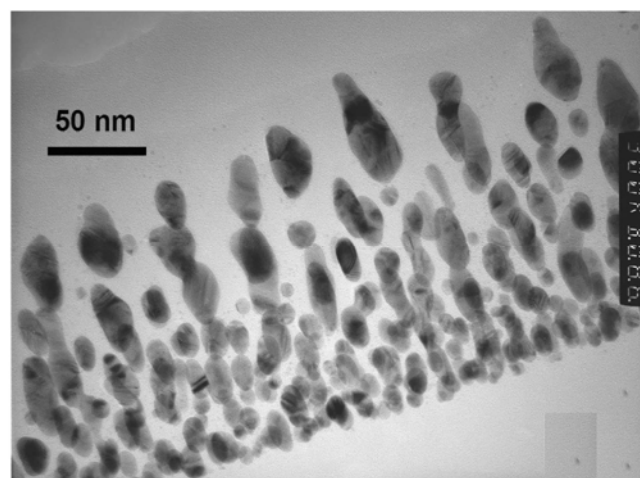


**Figure 13.** Cross-sectional TEM pictures show the Au nanoparticles in pristine and irradiated Au–silica nanocomposite<sup>63</sup>.

bombardment conditions<sup>64</sup>. Now while irradiating still smaller particles (diameters of 0.25–2 nm) with low volume fractions (1–5%) by Ag or Au ions of 100 MeV, we observed a dissolution of the particles, indicating that the quenching rate from the melt after thermal spikes is so fast that Ag atoms do not find time for gathering into fresh nanoclusters despite their low solubility in silicate glasses<sup>42</sup>. When using ions of quite low energies (1–3 MeV) for irradiating the same films, the growth of these small particles was evidenced by the sharpening of their SPR peak. Since such ions produce no spike, the growth was attributed to the ionization of Ag atoms located at the surface of Ag clusters followed by their migration until a new interface to precipitate was found. Statistically, this process contributes to the ripening of particles with a lower surface/volume ratio.

The irradiation of Au nanoparticles with thick silica shells (a colloid deposited on a surface) gave the interesting result that the silica shells get flattened, perpendicular to the incident ion direction, whereas the Au particles became elongated along the ion beam direction<sup>65</sup>. The flattening of the silica particles was an ideal case of the hammering effect of ions on amorphous targets at very high fluences modelled by Klaumünzer<sup>66</sup>. It consists of some kind of viscoelastic flow of the material leading to an increase of density parallel to the ion beam direction or in the jargon of glasses specialists, a redistribution of the free volume which constitute the partial point defects in amorphous solids. The silica material during its expansion causes a pressure to the Au particle squeezing it in a plane perpendicular to the ion beam, provided that the ratio of silica over Au radii in the core-shell colloid is large enough.

#### *Effect of SHI irradiation on nanoparticles of magnetic transition metals in silica*

Normally the magnetization of a thin film parallel to the surface is easier than in a film perpendicular to it because of the shape anisotropy: the hysteresis  $M(H)$  curves are more squared and residual magnetization under zero applied field is larger parallel to the surface. For application in magnetic recording with high density, an easy axis of magnetization perpendicular to the surface is desirable. It has been shown that this could be achieved for silica films embedded with small Fe particles (mean diameter 7 nm) with a low volume fraction (7%) by irradiation with SHI<sup>43,67</sup>. This was explained on the basis of the stress exerted on the nanoparticles by the matrix, due to the hammering effect of SHI on amorphous targets discussed earlier. Indeed no alignment of the Fe nanoparticles nor the formation of Fe nanowires, modifying the shape anisotropy was observed by TEM. This change in the orientation of easy magnetization is put into evidence more easily by means of electron spin resonance (ESR)

than by magnetization tests, since in ESR experiments the angular dependence of the magnetization under zero applied field is determined easily and given by well-known equations. The resonance field is minimum parallel to the easy axis, which is parallel to the surface in pristine films and becomes perpendicular to it after irradiation with  $10^{13}$  Au ions of 100 MeV as shown in Figure 14 for a silica film containing 3 vol% of super paramagnetic Fe nanoparticles with a size of  $\sim 5$  nm. Similar out of plane magnetic anisotropy was induced by SHI irradiation for particles of FePt  $L_{10}$  with comparable sizes and volume fractions<sup>68</sup>. It was attributed to an elongation of the nanoparticles along the beam direction.

The effect of swift ions on magnetic metals in solid solution or in the form of particles in same silica matrix depends on the content of magnetic metal and initial size of particles in pristine films. The magnetic transition metals are much more soluble in silica and glasses than noble metals, and thin films deposited by co-evaporation or sputtering with as high atomic contents of Fe as 10% is in solid solution in  $\text{SiO}_2:\text{Fe}$ . It has been shown that ion irradiation of such films is more efficient than thermal treatments at high temperatures (over  $900^\circ\text{C}$ ) under reducing atmosphere for promoting a reduction and precipitation of Fe in silica films<sup>59,66–68</sup>. When the metal is already precipitated (for metal volume fraction is larger than 10%), SHI irradiation does not affect the magnetization anisotropy by magnetostriction. However, a strong increase of coercivity is recorded when the external field is applied parallel to the surface.

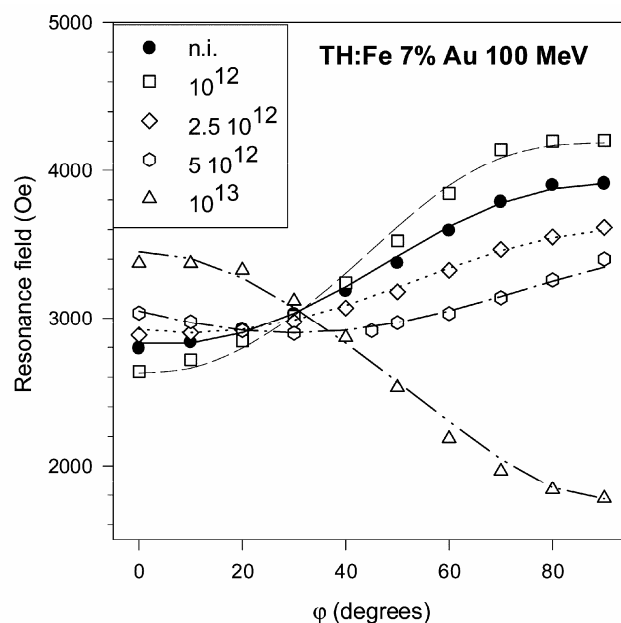


**Figure 14.** Plot of variation of the electron spin resonance (ESR) field as a function of the angle  $\phi$  between the field and the surface, is shown, for silica containing 7 at% Fe irradiated with 100 MeV Au ions, at fluences indicated in the frame (n.i. is for non irradiated). The tilt of easy magnetization axis (corresponding to the minimum field) is shown with ion fluence<sup>67</sup>.

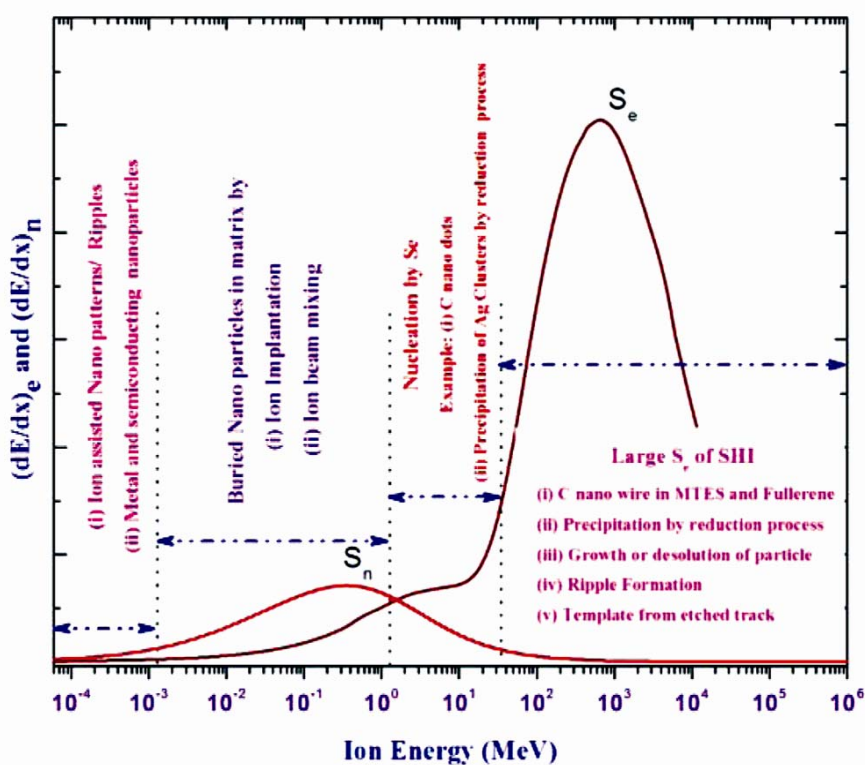


**Figure 15.** Sketch shows the role of ions in different energy regimes in nanostructuring the materials.  $S_e$  and  $S_n$  represent  $(dE/dx)_e$  and  $(dE/dx)_n$  respectively.

### Other systems

There have also been studies of the effect of SHI irradiation on nanoparticles of copper oxide and ZnS in silica, showing the capability of modifying the particle size and distribution by SHI irradiation<sup>69,70</sup>. More experiments and simulations are required in the case of semiconducting particles in silica or other insulating matrices.

From the experiments discussed in various sections, it is evident that the energetic ions may play a crucial role in synthesizing nanostructures (discussed from the second sections onwards) as well as in modifying the nanostructures in different energy regimes (discussed in this section) as shown in Figure 15. The applications of focused ion beams of a few tens of keV, a new emerging tool in creation of nanostructures is not covered in this article.

### Conclusion

The applications of ion beams in different energy regimes, to create or modify nanostructures was discussed on basis of a large number of experiments, most of which are performed at IUAC and CSNSM. Atom beams of few keV can be used to synthesize nanocomposites or to create ripples at the surface. The implantation and ion beam mixing with a few hundred keV ions are useful for obtaining buried nanoparticles. Irradiation with SHI of

polymers or fullerenes were shown to produce precipitations of carbon nanoparticles and nanowires. The modification of the size and shape of metal nanoparticles in an insulating matrix has been discussed in terms of thermal spikes and hammering effects.

1. International Conference on 'Advanced Nano Materials', Aveiro, Portugal, 22–25 June 2008.
2. International Conference on Nanomaterials and Nanomanufacturing, Dublin, 17 and 18 December 2007; International Conference on Multifunctional Nanocomposite and Nanomaterials, Egypt, 11–13 January 2008.
3. International Conference on Nanoscience and Technology (ICONSAT 2006), IIT Delhi, New Delhi, India, 16–19 March 2006 and March 2010, IIT Bombay; Avasthi, D. K. and Bolse, W. (eds), In Proceedings of Indo German Workshop on Synthesis and Modification of Nanostructures by Ion Beam, published in *Nucl. Instr. Meth. B*, March 2006.
4. Wang, Z. G., Dufour, Ch., Paumier, E. and Toulemonde, M., The  $S_e$  sensitivity of metals under swift-heavy-ion irradiation: a transient thermal process. *J. Phys.: Condens. Matter*, 1994, **6**, 6733–6750.
5. Ziegler, Z. F. and Biersack, J. P. ([www.srim.org](http://www.srim.org)).
6. Rusponi, S., Costantini, G., Boragno, C. and Valbusa, U., Ripple structure on Ag(110) surface induced by ion sputtering. *Phys. Rev. Lett.*, 1997, **78**, 2795–2798; Rusponi, S., Costantini, G., Boragno, C. and Valbusa, U., Ripple wave vector rotation in anisotropic crystal sputtering. *Phys. Rev. Lett.*, 1998, **81**, 2735–2738.
7. Cuerno, R., Makse, H. A., Tomassone, S., Harrington, S. T. and Stanley, H. E., Stochastic model for surface erosion via ion sputtering: dynamical evolution from ripple morphology to rough morphology. *Phys. Rev. Lett.*, 1995, **75**, 4464–4467.

8. Kulriya, P., Tripathi, A., Kabiraj, D., Khan, S. A. and Avasthi, D. K., Study of 1.5 keV Ar atoms beam induced ripple formation on Si surface by atomic force microscopy. *Nucl. Instr. Meth. B*, 2006, **244**, 95–99.
9. Paramanik, D. and Verma, S., Pattern formation on InP(111) surfaces after ion implantation. *Nucl. Instr. Meth. B*, 2006, **244**, 69–73; Karmakar, P. and Ghose, D., Ion beam sputtering induced ripple formation in thin metal films. *Surf. Sci.*, 2004, **554**, L101–L106; Karmakar, P., Mollick, S. A., Ghose, D. and Chakrabarti, A., Role of initial surface roughness on ion induced surface morphology. *Appl. Phys. Lett.*, 2008, **93**, 103102–103105.
10. Chini, T. K., Sanyal, M. K. and Bhattacharya, S. R., Energy-dependent wavelength of the ion-induced nanoscale ripple. *Phys. Rev.*, 2002, **66**, 153044–153408.
11. Kabiraj, D., Abhilash, S. R., Vanmarcke, L., Cinausero, N., Pivin, J. C. and Avasthi, D. K., Atom beam sputtering setup for growth of metal particles in silica. *Nucl. Instr. Meth. B*, 2006, **244**, 100–104.
12. Mishra, Y. K., Mohapatra, S., Kabiraj, D., Mohanta, B., Lalla, N. P., Pivin, J. C. and Avasthi, D. K., Synthesis and characterization of Ag nanoparticles in silica matrix by atom beam sputtering. *Scr. Mater.*, 2007, **56**, 629–632.
13. Singhal, R., private communication.
14. Avasthi, D. K., Mishra, Y. K., Kabiraj, D., Lalla, N. P. and Pivin, J. C., Synthesis of metal–polymer nanocomposite for optical applications. *Nanotechnology*, 2007, **18**, 125604–125608.
15. Mishra, Y. K., Mohapatra, S., Singhal, R., Avasthi, D. K., Agarwal, D. C. and Ogale, S. B., Au–ZnO: a tunable localized surface plasmonic nanocomposite. *Appl. Phys. Lett.*, 2008, **92**, 043107–043110.
16. Hutchings, G., *Catalysts*, 2004, **34**.
17. Schuberty, Ch., Wesh, W., Kaiser, U., Heldler, A., Gartner, K., Gorelik, T. and Glatzel, U., Synthesis of group IV nanocrystals in SiC by ion beam processing. *Nucl. Instr. Meth. B*, 2002, **191**, 428–432.
18. Giri, P. K., Kesavamoorthy, R., Panigrahi, B. K. and Nair, K. G. M., Studies on the formation of Si nanocrystals in SiO<sub>2</sub> by Ge ion implantation. *Nucl. Instr. Meth. B*, 2006, **244**, 56–59.
19. Amrithapandian, S. *et al.*, Formation of Fe nanoclusters embedded in Ge and irradiation induced amorphisation and crystallisation of Fe<sup>+</sup> ion implanted Ge. *Nucl. Instr. Meth. B*, 2006, **244**, 52–55.
20. Zheng, N. P., Pivin, J. C. and Ruault, M. O., Epitaxial growth of nitrides in Ti implanted with N. *Europhys. Lett.*, 1988, **8**, 689–694.
21. Pivin, J. C., Zheng, P. and Ruault, M. O., *Philos. Mag. Lett.*, 1989, **59**, 25; Pivin, J. C., Zheng, P. and Ruault, M. O., Transmission electron microscopy investigation of the structural transformations in titanium or TiAl implanted with nitrogen, carbon, oxygen and boron. *Mater. Sci. Eng. A*, 1989, **115**, 83–88.
22. White, C. W. *et al.*, Encapsulated semiconductor nanocrystals formed in insulators by ion beam synthesis. *Nucl. Instr. Meth.*, 1998, **141**, 228–240.
23. Gao, Y., Wong, P. S., Cheung, W. Y., Shao, G. and Homewood, K. P., Characterization and light emission properties of  $\beta$ -FeSi<sub>2</sub> precipitates in Si synthesized by metal vapor vacuum arc ion implantation. *Nucl. Instr. Meth. Phys. Res. B*, 2003, **206**, 317–320.
24. Pivin, J. C., Use of ion beams to produce or modify nanostructures in materials. In *Nanomaterials: New Research* (ed. Caruta, B. M.), Nova Science Publishers Inc, 2005, chapter 2, pp. 81–113.
25. Mazzoldi, P., Tramontin, L., Boscolo-Boscoletto, A., Battaglin, A. and Arnold, G. W., Substrate effects in silver-implanted glasses. *Nucl. Instr. Meth. Phys. Res. B*, 1993, **80/81**, 1192–1196.
26. Battaglin, G., Cattaruzza, E., D'Acapito, F., Gonella, F., Mazzoldi, P., Mobilio, S. and Priolo, F., EXAFS study on metal cluster doped silica glass obtained by ion implantation procedures. *Nucl. Instr. Meth. Phys. Res. B*, 1998, **141**, 252–255.
27. Pivin, J. C., Garcia, M. A., Liopis, J. and Hofmeister, H., Interaction between clusters in ion implanted and ion beam mixed SiO<sub>2</sub>: Ag films. *Nucl. Instr. Meth. B*, 2002, **191**, 794–799.
28. Mohanty, T., Pradhan, A., Gupta, S. and Kanjilal, D., Nanoprecipitation in transparent matrices using an energetic ion beam. *Nanotechnology*, 2004, **15**, 1620–1624.
29. Pivin, J. C., Malinivoska, D. D., Sendova Vassileva, M. and Nikolaeva, M., Mixing of metals in Si with 4.5 MeV Au ions. *Nucl. Instr. Meth. B*, 2001, **174**, 453–462.
30. Pivin, J. C. *et al.*, Optical properties of silver clusters formed by ion irradiation. *Eur. Phys. J.*, 2002, **20**, 251–260.
31. Pivin, J. C., Mixing of noble metals in oxides and formation of colloids by ion irradiation. *Mater. Sci. Eng. A*, 2000, **293**, 30–38.
32. Pivin, J. C., Garcia, H. A., Llopis, J. and Hofmeister, H., Interaction between clusters in ion implanted and ion beam mixed SiO<sub>2</sub>: Ag films. *Nucl. Instr. Meth. B*, 2002, **191**, 734.
33. Davenas, J., *Solid State Commun.*, 1993, **30–31**, 317.
34. Venkatesan, T., High energy ion beam modification of polymer films. *Nucl. Instr. Meth. B*, 1985, **7–8**, 461–462.
35. Venkatesan, T. *et al.*, In *Ion Beam Modification of Insulators* (eds Mazzoldi, P. and Arnold, G. W.), Elsevier, Amsterdam, 1987, p. 301.
36. Pivin, J. C., Pippel, E., Woltersdorf, J., Avasthi, D. K. and Srivastava, S. K., Structural transformation induced by swift heavy ions in polysiloxanes and polycarbosilanes. *Z. Metall.*, 2001, **92**, 712.
37. Pivin, J. C., Avasthi, D. K., Singh, F., Kumar, A., Pippel, E. and Sagon, G., Precipitation of C, Si and metals nanoparticles in silicon-based gels induced by swift heavy ion irradiation. *Nucl. Instr. Meth. B*, 2005, **236**, 73–80.
38. Kumar, A., Singh, F., Pivin, J. C. and Avasthi, D. K., Fabrication of carbon nanostructures (nanodots, nanowires) by energetic ion irradiation. *J. Appl. Phys. D*, 2007, **40**, 2083–2088.
39. Seki, S., Maeda, K., Tagawa, S., Kudoh, H., Sugimoto, M., Morita, Y. and Shibata, H., Formation of nanowires along ion trajectories in Si backbone polymers. *Adv. Mater.*, 2001, **13**, 1663–1665; Pivin, J. C., Vincent, E., Esnouf, S. and Dubus, M., Magnetic properties of Fe and Ni nanoparticles formed in triethoxysilane films by ion irradiation or thermal processing. *Eur. Phys. J. B*, 2004, **37**, 329–337.
40. Gibbson, J. F., Ion implantation in semiconductors – Part II: Damage production and annealing. *Proc. IEEE*, 1972, **60**, 1062.
41. Pivin, J. C., Ion induced precipitation of metal particles in triethoxysilane for optical and magnetic applications. *Nucl. Instr. Meth. B*, 2003, **216**, 239–244.
42. Pivin, J. C., Roger, G., Garcia, M. A., Singh, F. and Avasthi, D. K., Nucleation and growth of Ag clusters in silicate glasses under ion irradiation. *Nucl. Instr. Meth. B*, 2004, **215**, 373–384.
43. Sigh, F., Avasthi, D. K., Angelov, O., Berthet, P. and Pivin, J. C., Changes in volume fraction and magnetostriction of iron nanoparticles in silica under swift heavy ion irradiation. *Nucl. Instr. Meth. B*, 2006, **245**, 214–218.
44. Pivin, J. C., Singh, F., Mishra, Y. K., Avasthi, D. K. and Stoquert, J. P., Synthesis of silica : metals nanocomposites and modification of their structure by swift heavy ion irradiation. *Surf. Coat. Technol.*, 2009, **203**, 2432–2435.
45. Chaudhari, P. S., Bhave, T. M., Kanjilal, D. and Bhoraskar, S., Swift heavy ion induced growth of nanocrystalline silicon in silicon oxide. *J. Appl. Phys.*, 2003, **93**, 3486–3490.
46. Tripathi, A., Kumar, A., Kabiraj, D., Khan, S. A., Baranwal, V. and Avasthi, D. K., SHI induced conducting tracks formation in C<sub>60</sub>. *Nucl. Instr. Meth. B*, 2006, **244**, 15–18; Tripathi, A., Kumar, A., Singh, F., Kabiraj, D., Avasthi, D. K. and Pivin, J. C., Ion irradiation induced surface modification studies of polymers using SPM. *Nucl. Instr. Meth. B*, 2005, **236**, 186–194.
47. Kumar, A., Avasthi, D. K., Tripathi, A., Kabiraj, D., Singh, F. and Pivin, J. C., Synthesis of confined electrically conducting carbon

- nanowires by heavy ion irradiation of fullerene thin film. *J. Appl. Phys.*, 2007, **101**, 014308–014313.
48. Kumar, A., Avasthi, D. K., Tripathi, A., Filip, L. D., Carey, J. D. and Pivin, J. C., Formation and characterization of carbon nanowires. *J. Appl. Phys.*, 2007, **102**, 044305–044309.
49. Martin, C. R., Controlling ion-transport selectivity in gold nanotubule membranes. *Adv. Mater.*, 2001, **13**, 1351–1362.
50. Ohgai, T., Hoffer, X., Gravier, L., Wegrowe, J. E. and Ansermet, J. P., Bridging the gap between template synthesis and microelectronics: spin-valves and multilayers in self-organized anodized aluminium nanopores. *Nanotechnology*, 2003, **14**, 978–982.
51. Wade, T. L. and Wegrowe, J. E., Template synthesis of nanomaterials. *Eur. Phys. J. – Appl. Phys.*, 2005, **29**, 3–22.
52. Ferain, E. and Legras, R., Track-etch templates designed for micro- and nanofabrication. *Nucl. Instr. Meth. Phys. Res. B*, 2003, **208**, 115–122.
53. Chawla, S., Ghosh, A. K., Avasthi, D. K., Kulriya, P. and Ahmad, S., Functionalization of industrial polypropylene films via the swift-heavy-ion-induced grafting of glycidyl methacrylate. *J. Appl. Polym. Sci.*, 2007, **105**, 3578–3587.
54. Rao, V. V., Amar, J. V., Avasthi, D. K. and Charlu, R. N., Etched ion track polymer membranes for sustained drug delivery. *Radiat. Measure.*, 2003, **36**, 585–589.
55. Chauhan, R. S. *et al.*, Presented in ANM 2007, IIT Mumbai, January 2007; Chauhan, R. S. and Agarwal, D. C., Surface nanostructuring of oxide thin films under MeV heavy ion irradiation. In *Nanostructuring by Energetic Ions* (eds Avasthi, D. K. and Pivin, J. C.), Nova Science Publishers, USA.
56. Bolse, W., Schattat, B. and Feyh, A., Modification of thin-layer systems by swift heavy ions. *Appl. Phys. A*, 2003, **77**, 11–15; Bolse, W., Self-organized nano-structuring of thin oxide films under swift heavy ion bombardment. *Nucl. Instr. Meth. Phys. Res. B*, 2006, **244**, 8–14.
57. Pivin, J. C., Singh, F., Kumar, A., Patel, M. K., Avasthi, D. K. and Dimova-Malinovska, D., Some structural modifications at the nanometric scale at the nanometric scale induced by swift heavy ion irradiation. In *Nanostructured Materials for Advanced Technological Applications* (eds Reithmaier, J. P. *et al.*), NATO Science Series B, Physics and Biophysics, Springer, Dordrecht, Netherlands, 2009, pp. 145–151.
58. Biswas, A. *et al.*, Nanoparticle architecture in carbonaceous matrix upon swift heavy ion irradiation of polymer–metal nanocomposites. *Nucl. Instr. Meth. B*, 2004, **217**, 39–50.
59. Singh, F., Ph D thesis, Paris University, 2007.
60. Kuri, P. K., Joseph, B., Lenka, H. P., Sahu, G., Ghatak, J., Kanjilal, D. and Mahapatra, D. P., Observation of a universal aggregation mechanism and a possible phase transition in Au sputtered by swift heavy ions. *Phys. Rev. Lett.*, 2008, **100**, 245501–245505.
61. Gupta, A. and Avasthi, D. K., Large electronically mediated sputtering in gold films. *Phys. Rev. B*, 2001, **64**, 155407–155412.
62. Mishra, Y. K. *et al.*, Controlled growth of gold nanoparticles induced by ion irradiation: an *in situ* X-ray diffraction study. *Appl. Phys. Lett.*, 2007, **90**, 73110–73113.
63. Mishra, Y. K., Singh, F., Pivin, J. C. and Avasthi, D. K., Synthesis of elongated Au nanoparticles in silica matrix by ion irradiation. *Appl. Phys. Lett.*, 2007, **91**, 063103–063106.
64. Penninkhof, J. J., Polman, A., Sweatlock, L. A., Maier, S. A., Atwater, H., Vredenberg, A. M. and Kool, B. J., Mega-electron-volt ion beam induced anisotropic plasmon resonance of silver nanocrystals in glass. *Appl. Phys. Lett.*, 2003, **83**, 4137–4139.
65. Roorda, S., Dillen, T. V., Polman, A., Graf, C., Blaaderen, A. V. and Kooi, B. J., Aligned gold nanorods in silica made by ion irradiation of core-shell colloidal particles. *Adv. Mater.*, 2004, **16**, 235–237.
66. Klaumünzer, S., Li, C. L., Löffler, S., Rammensee, M., Schumacher, G. and Neitzer, H. C., *Rad. Eff. Def. Sol.*, 1989, **108**, 131.
67. Pivin, J. C., Esnouf, S., Singh, F. and Avasthi, D. K., Investigation of the precipitation kinetics and changes of magnetic anisotropy of iron particles in ion-irradiated silica gel films by means of electron-spin resonance. *J. Appl. Phys.*, 2005, **98**, 023908–023914.
68. Pivin, J. C., Singh, F., Angelov, O. and Vincent, L., Perpendicular magnetization of FePt particles in silica induced by swift heavy ion irradiation. *J. Phys. D: Appl. Phys.*, 2009, **42**, 025005–025011.
69. Balamurugan, B. *et al.*, Modifying the nanocrystalline characteristics – structure, size, and surface states of copper oxide thin films by high-energy heavy-ion irradiation. *J. Appl. Phys.*, 2002, **92**, 3304.
70. Mohanta, D., Nath, S. S., Mishra, N. C. and Choudhury, A., Irradiation induced grain growth and surface emission enhancement of chemically tailored ZnS:Mn/PVOH nanoparticles by  $\text{Cl}^{19}$  ion impact. *Bull. Mater. Sci.*, 2003, **26**, 289–294.

ACKNOWLEDGEMENTS. We thank the Indo French Centre for Promotion of Advanced Research (IFCPAR), New Delhi for its financial support to the project ‘Nano phase generation by energetic ion beams’ and to the DST, New Delhi for providing financial support to the projects ‘Intensifying research in high priority areas (IRHPA)’, New Delhi, and ‘Nanostructuring by ion beams’ under Nano Mission initiative. We also thank all our collaborators, D. Kabiraj, A. Tripathi, F. Singh, A. Kumar, Y. K. Mishra, D. C. Agarwal and R. Singhal who actively contributed to our research work.

Received 2 March 2008; revised accepted 11 February 2010